Analysis the Surface Morphology of the Porous Media by using Atomic Force Microscope technique

Bashir Y. Sherhan Al-Zaidi

Department of Chemical Engineering/ University of Technology/ Membrane Technology Research
Email: 80193@uotechnology.edu.iq

Abstract

An atomic force microscope (AFM) technique is utilized to investigate the polystyrene (PS) impact upon the morphological properties of the outer as well as inner surface of poly vinyl chloride (PVC) porous fibers. Noticeable a new shape of the nodules at the outer and inner surfaces, namely "Crater nodules", has been observed. The fibers surface images have seen to be regular nodular texture at the skin of the inner and outer surfaces at low PS content. At PS content of 6 wt.%, the nodules structure was varied from Crater shape to stripe. While with increasing of PS content, the pore density reduces as a result of increasing the size of the pore at the fiber surface. Moreover, the test of 3D-AFM images shows that the roughness of both surfaces of fibers seems to be decreased with PS content. Alternatively, the fibers pure water permeability (PWP) has been declined with decreasing of fiber roughness.

Keywords: Polymeric surface; porous surface; Additive; surface morphology; AFM .

1. Introduction

Today, AFM is used with extremely range of applications; from normal fantasy of morphology to advanced inspection of surface properties at the array of sub-nanometer [1]. The nodules and nodular aggregates size in addition to the roughness and size of the pore with dispersion of the pore diameter would be able to measure via AFM technique [2-14]. The pore sizes of the polysulfone (PSF) surface were measured through AFM and scanning electron microscope (SEM) techniques by means of researchers Kim and co-workers [4]. They observed that the AFM was more precise in comparison with the results obtained by SEM technique. Moreover, pore diameter, nodule size and roughness of PSF fibers surface were also evaluated by Rafat et al. [5] using SEM and AFM techniques. Barzin et al., and Otero et al. [6,9] had tested the surface roughness of polyether sulfone, PES fibers, through AFM technique. While the roughness and the size of nodular for external surface of cellulose acetate

butyrate, CAB fiber, had previously been tested [13]. Furthermore, a new method to analyze the extracted data from the AFM images using Matlab software was found by El-Hadidy et al. [14]. Additionally, Razali et al [15] achieved the distribution of the pore diameter of PES / polyaniline (PANI) nano-particles membranes by AFM technique. Concerning the specification and characterization of the structural morphology of the membrane that might be utilized for membrane distillations applications, Shirazi et al. [16] had used AFM technique for measuring the roughness, diameter, and distribution of the pore diameter of membrane separated from various hydrophobic polymeric materials. According to the importance of the structural morphology (i.e., membrane roughness) on the performance of the fibers, which it means membrane with low fouling, the membrane properties were investigated in this work. Some researchers focused their work on the impact of the roughness of the membranes on the performance, for example, Chunget. al., [17] had demonstrated the shear rate impact on the PES

morphology of ultrafiltration (UF) membranes by using AFM. It was reported that the pure water flux of the membranes was proportional to the mean roughness, as the lower mean roughness was led to higher separation factor. From the preceding effort, improvement in hollow PVC/PS fibers permeability was also investigated by using AFM technique [18]. Plenty of workers were utilized the AFM technique for measuring the characteristic of the fiber surface, but indeed the workers didn't show the sufficient concern of AFM technique in their efforts. Thus, the significant goal of this effort is to inspect the impact of PS content in blend solution through the use of AFM technique on fiber surface properties.

2. Experimental Procedure
2.1. Blend Hollow Fiber

PVC-PS Fibers with different PS contents (1 to 6% by weight) at14 wt% PVC with dimethylacetamide (DMAC) as solvent were used in the present work and assigned as PS1, PS2, PS3, PS4 and PS6. The parameters and conditions of the spinning process of the fibers and all details were explained elsewhere [18].

2.2 Fibers permeability (PWP)

PWP of the fibers was commonly evaluated after constructed of the fibers cells. Each cell has six fibers of 20 cm long. Ends of the cell of fibers bundles might be agglutinant by utilizing an epoxy resin into two stainless steel tees. Figure 1 presents the ultra-filtration (UF) system. By using 1 bar as a trans-membrane pressure and 26°C temperature of de-ionized water, the experiments were orderly achieved in fibers cell. PWP could be evaluated utilizing the operating correlation below:

$$PWP = \frac{Q_w}{\Delta P \, A} \qquad \ldots (1)$$

Where ΔP is the pressure gradient across the fiber (bar), and A is effective area of fibers (m^2), and Q_w is the volumetric flow rate (l/h).
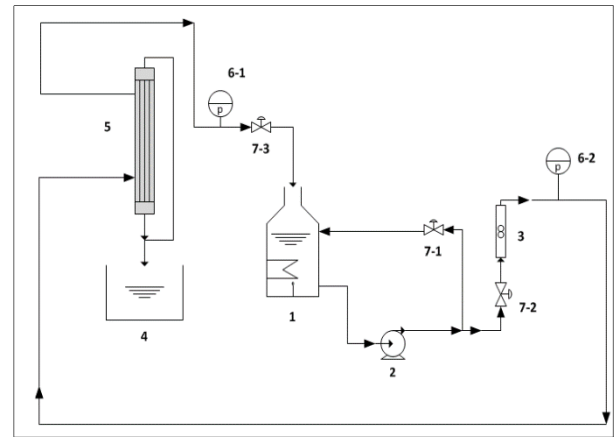

Fig. 1. Schematic diagram of the UF membrane experimental unit; 1: Feed tank, 2: Pump, 3: Flow meter, 4: Permeate tank, 5: Hollow fiber module, 6-1, 2: Gauge pressure, 7-1, 2, 3: Valve.

2.3. Fiber Characteristic by AFM-Technique

By employing an AFM (Angstrom Advanced Inc., AA3000 model (USA)) and the use of contact mode through appropriate tip (made from silicon material), the blend fibers might succumb to the surface analysis. The measurements were inclusive an assessment of the topography and the profiling force as well as deflection and its amount. The software IMAGER version 4.31 was exercised to evaluate the statistical distribution of the pore diameter for the outer fibers surfaces. In addition, depending on the AFM results, roughness parameters could be estimated. Based on these different roughness parameters, the surfaces of the blend fiber were inspected, for instance, the root mean square of Z values [R_{ms}(nm)], the mean roughness [R_a(nm)], the vertical space between the lowest ravines, and also the highest peaks [R_{max}]. Fibers roughness is important features of the surface of the fiber, where it owns a strong impact on fouling as well as concentration polarization of the fibers, as it had demonstrated by Chung et. al. [17].

The standard shifting of pixel amounts from the plane are introduced as the mean roughness, also it could be estimated via utilizing the correlation below:

$$R_a = 1/l_X \, l_Y \left[\int_0^{l_Y} \int_0^{l_X} |f(X,Y)| dX dY \right] \qquad \ldots (2)$$

Here $f(X,Y)$ means the surface relating toward the center of the plane, also l_Y and l_X were define as a surface dimensions. R_{ms} (nm) is surface roughness that could either be measured statistically or be estimated theoretically as the

shifting of all pixel amounts from the mean pixel amount $\bar{Z}$ as follows:

$$R_{ms} = \sqrt{\frac{\sum\limits_{\substack{X=1,i \\ Y=1,j}} \left(\bar{Z} - Z_{X,Y}\right)^2}{(j-1)(i-1)}} \qquad ... (3)$$

Here $Z_{X,Y}$ is the height image pixel respect to the height of the plane center $\bar{Z}_{X,Y}$ and i and j are the pixels number in the directions of $X\&Y$ [19].

It is important to saying that the fiber mean roughness is a relative value owing to the reliance of the roughness on the bending [20].

3. Results and Discussion
3.1 AFM Analysis

AFM pictures with 3-dimensional and 2-dimensional view of the inner surface at 2.065 µm x 2.065 µm fibers area are presented in Figure 2. Crater nodules could be observed with different sizes at the inner surface, and this shape of nodules was not mentioned yet in the literature. Also, the Crater nodules were semi-regularly appeared on the surface as presented in Figure 2a to Figure 2c. Furthermore, the size of the Crater nodules at the inner surface were increased with increasing of PS content in the blend solution to 3 wt.%. More rising of PS content such as, 4 and 6 wt.% is result to the nodules nip up with each other, therefore, new nodules shape could be observed on the fiber surfaces, namely "stripe". The nodules in the shape of stripe are randomly distributed among the nodules with Crater shape as depicted in Figures 2d and 2e. Moreover, AFM pictures with 3-dimensional and 2-dimensional view of the outer surface at area of 2.065 µm x 2.065 µm for fibers made by using different PS contents in blend solution is presented in Figure 3. The nodules in Crater shape are become visible with increasing the PS content from 1 to 3 wt.% in blend solution as illustrated in Figures 3a, 3b and 3c. More mounting in PS content up to 4 wt.% within blend solution is results in combination of the nodules [see Figure 3d]. PS with content of 6 wt.%, results to completely turn out the nodules structure in the shape of the Crater to the nodules in the shape of stripe as it can be distinguished in Figure 3e.
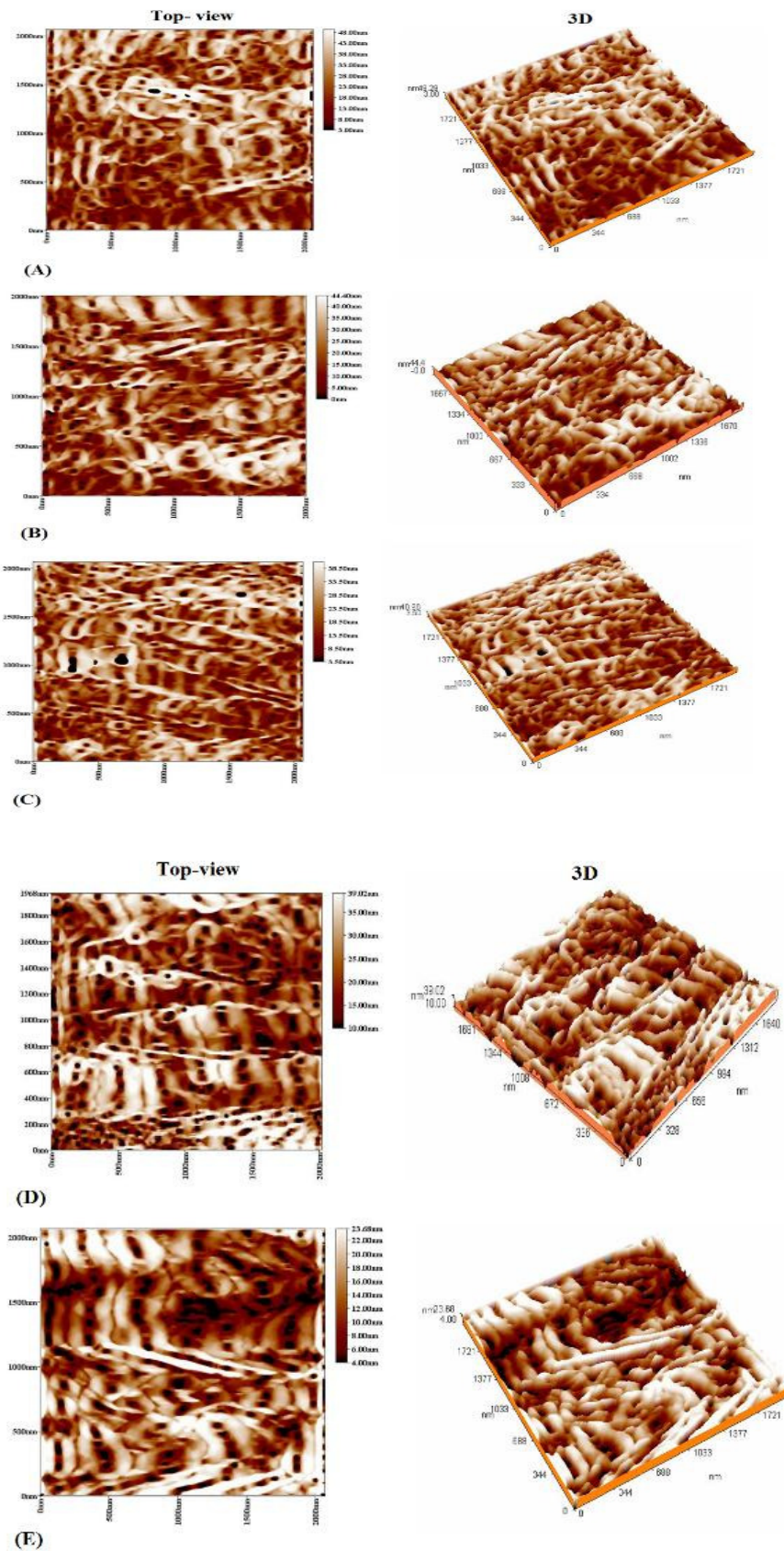
Fig. 2. Three-dimensional and top view AFM pictures of the inner surface of the hollow fiber blend membranes: (A) PS1, 1 wt.%, (B) PS2, 2 wt.%, (C) PS3, 3 wt.%, (D) PS4, 4 wt.%, (E) PS6, 6 wt.%.
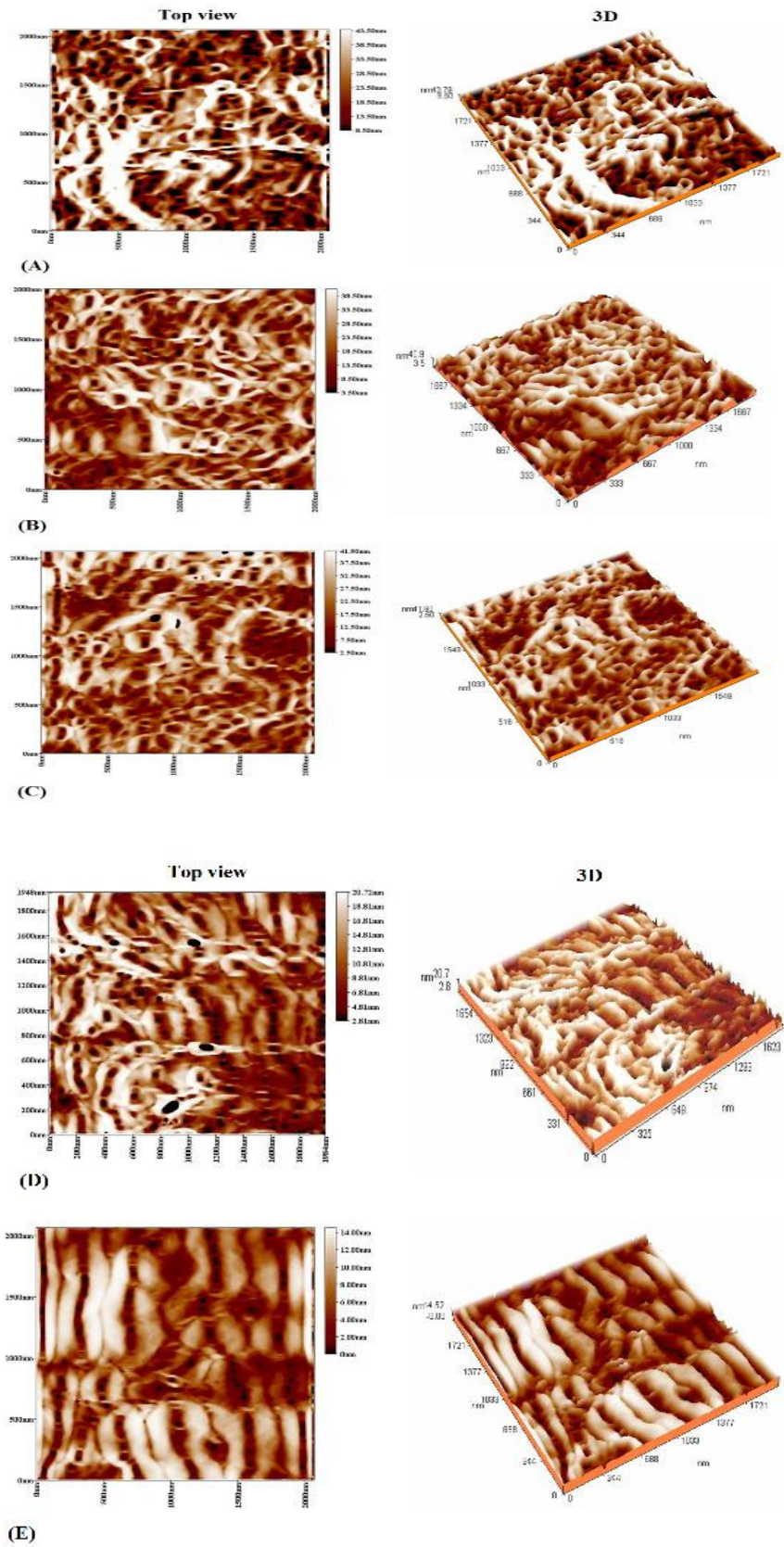
101

Fig. 3. Three-dimensional and top view AFM pictures of the outer surface of the hollow fiber blend membranes: (A) PS1, 1 wt.%, (B) PS2, 2 wt.%, (C) PS3, 3 wt.%, (D) PS4, 4 wt.%, (E) PS6, 6 wt.%.

The phenomenon behind such observation for outer and inner surfaces can be attributed to the exchange rate of the water from the internal and external coagulation baths with solvent (DMAC) in blend solution. The speed of the interchange rate is strongly dependent upon the difference in solubility parameter (SP) for PVC and PS with DMAC, for example, the variation in SP ($\Delta\delta$) between DMAC as well as PVC was found to be 7.5 (MPa)$^{0.5}$, whereas regarding DMAC as well as PS, the ($\Delta\delta$) was obtained to be 14.7 (MPa)$^{0.5}$ [21,22]. Freezing process of polystyrene (PS) throughout the nascent fiber formation seems to be faster than that of PVC. This phenomenon can be described from the other side according to the increment of PS content in blend solution, which leads to slow blend solution and water de-mixing process. On account of the variation in solubility parameter between DMAC with PVC and PS, the PS nodules combined with each other quicker in comparing with that can be observed in PVC nodules during the formation process of the fiber; hence the structure of the stripe nodules was nearly formed and spread regularly on the surface.

In fact, the mechanism of the phase separation has a significant effect on the morphological structure of fibers synthesized by the phase inversion technique [4,23]. By the phase separation method the polymer solution can be separated into two phases: polymer poor phase, that represents the cavities (e.g., pores); and polymer rich phase (membrane matrix). Here, the retard in the solvent-water de-mixing process can be take place throughout the configuration of the nascent fiber at the inner surface. Perhaps few amount of non-solvent (e.g., water) within internal coagulant was the main foundation for this phenomenon, which is guided to enhance of DMAC content through the internal coagulant and therefore led to obtain a layer with looser skin. While the instantaneous solvent-water de-mixing process could be occurred, ones the nascent fiber being into direct connection with the water at the outer surface (i.e., external coagulation bath). It is obvious that the phase separation is introduced as a converted for the polymer mixture into two phases; the first one concerning the rich phase (solidified polymer), which demonstrates the matrix of the membrane but the second concerning with polymer poor phase, which exhibits the sinus as it had already been reported by Kesting [23].

3.2. Pore and Pore Size Distribution

The mean diameter of the pore for both outer and inner surfaces of the blend fiber can be outlined

in Tables 1 and 2, and the pore density is also illustrated in Figure 4. The pore density is diminished while the mean pore size elevated with increasing of PS content in blend solution as shown in Figure 4. Principally, this behavior is due to the quantities of polymers in the blend solution. Increment in the viscosity of the blend solution with increasing of PS content led to delay the movement of the solvent in the blend solution toward the water. Consecutively, this behavior might be gone ahead to make low pore density and large pore size at the fiber surface.
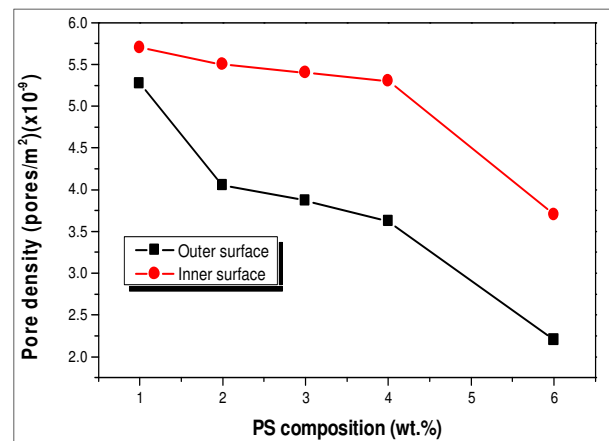

Fig. 4. Effect of PS compositions on the pore density of the hollow fiber blend membranes.

Furthermore, the blend process of DMAC as a solvent and both PS and PVC as a membrane blend can be classified as a homogeneous process since the two polymers have a non-polar character. As a consequence, it is possible to obtain a physical mixing of the polymers. This is the second reason might be backing the aforementioned observation [25]. Dong-liang et al. [25] had detected that an increase in the content of the polymer within the casting solution would be led to decrease the density of the pores.

Table 1,
Mean pore size and mean roughness of the inner surface of the hollow fiber blend membranes

Membrane code	PVC/PS/DMAC Solution (wt.%)	Mean pore size (nm)	Inner surface roughness (2065×2065 nm^2)		
			Mean roughness [1](R_a) (nm)	The root mean square of Z values [2](R_{ms}) (nm)	Maximum roughness [3](R_{max}) (nm)
PS1	14:1:85	104.16	10.7	12.4	45.2
PS2	14:2:84	109.28	10.2	11.9	43.9
PS3	14:3:83	138.16	8.45	9.87	36.9
PS4	14:4:82	140.82	7.64	8.86	28.9
PS6	14:6:80	195.98	5.47	6.30	19.1

[1] (R_a): The mean value of the surface relative to the center plane.
[2] (R_{ms}): The root mean square of Z values.
[2] (R_{max}): Maximum roughness (vertical distance between the highest peaks and the lowest valleys).

Table 2,
Mean pore size and mean roughness of the outer surface of the hollow fiber blend membranes.

Membrane code	PVC/PS/DMAC Solution (wt.%)	Mean pore size (nm)	Outer surface roughness (2065×2065nm^2)		
			Mean roughness (R_a) (nm)	The root mean square of Z values (R_{ms}) (nm)	Maximum roughness (R_{max})(nm)
PS1	14:1:85	109.19	10.5	12	35.1
PS2	14:2:84	117.86	8.64	10.1	34.6
PS3	14:3:83	141.12	7.12	9.6	32
PS4	14:4:82	142.86	4.47	5.19	17.8
PS6	14:6:80	184.48	3.48	4.03	14.2

Figure 5 presents the impact of PS content on the distribution size of the pores of fiber inner surface. The size distribution of the pores of the fibers is in the range of 75 and 205 nm, while the size frequency of the pores is in between of 75 and 85 nm, which is above 17.28% and 17% respectively of the prepared blend fibers from PS content of 1 wt.% as demonstrated in Figure 5. The distribution of the pore size of the synthesized fibers from PS of 2wt.% is in the range of 70 and 340 nm and the frequency of the pore sizes is 75, 85, and 95 nm, which is approximately 14, 12, and 11% respectively. More increment in the PS content of about 3 wt.%, makes the distribution of the pore size to be in the range of 120 and 210 nm and around 25.64% highest frequency of the 120 nm pore size as given in Figure 5. Likewise for PS content of about 4wt.% in blend solution, most pores are seen in the size of 110 nm and equivalent to frequency of 19%. Also for PS content of about 6 wt.%, the distribution of the pore size becomes in the range of 160 to 440 nm and in the size of 180 nm with 19% pores frequency is found in that case. In Figure 6, impact of PS content on distribution of the pore diameter of the fibers outer surface has been depicted. Here it can be seen that the distribution of the pore diameter is in the range of 70 to 310 nm and the frequency at pore size of 90 nm is about 25% for the prepared blend fiber with PS of 1 wt.% inside blend mixture.
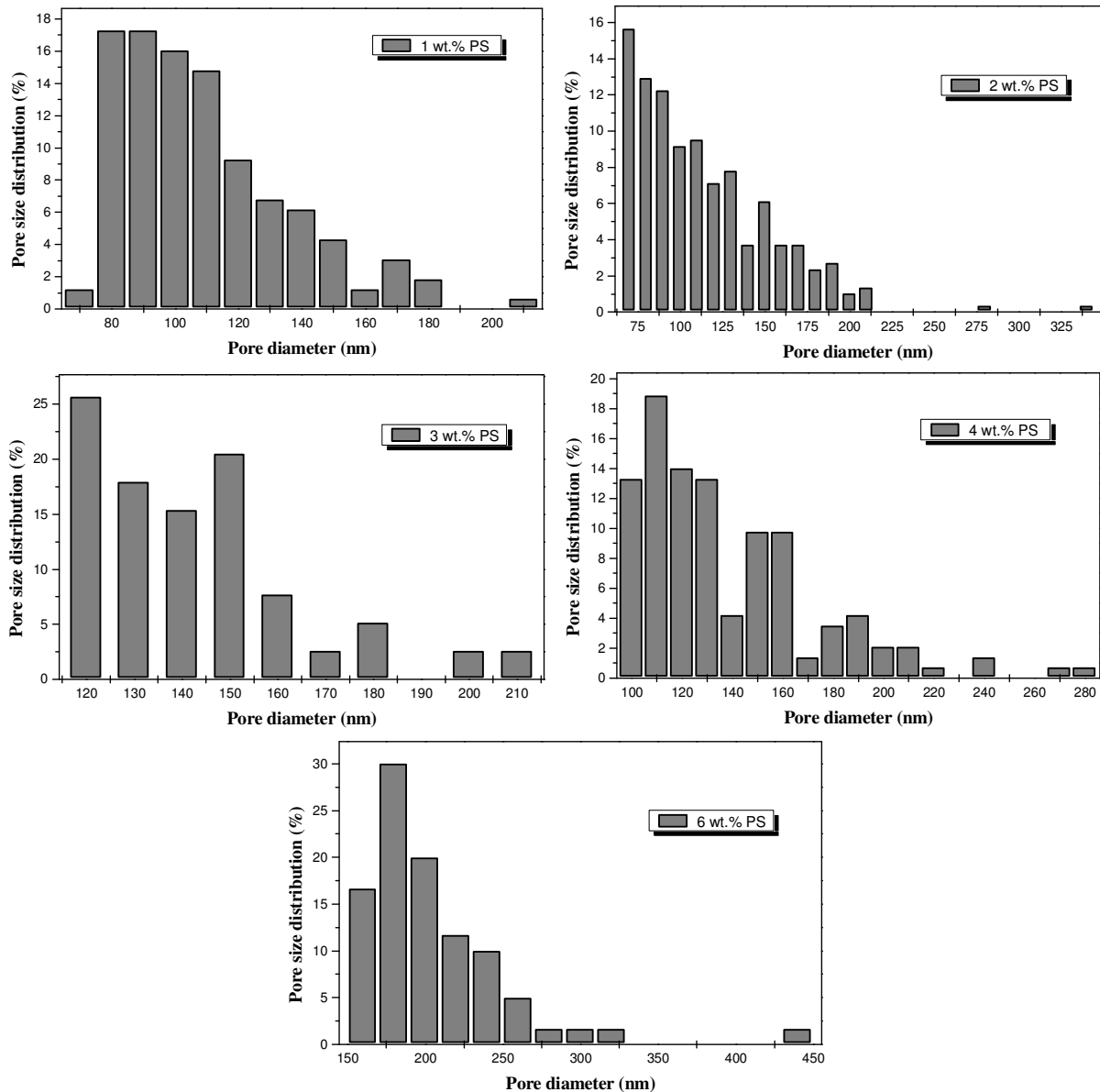
Fig. 5. Pore size distributions of the inner surface of the hollow fiber blend membranes.

Above and beyond, the size distribution of the pores transferred to the right and initiated of 95 to 175 nm as well as the frequency of the pore size at 110 nm is approximately 18.44%, as a result of the rising the content of PS to 2 wt.%. For PS content 3 wt.%, the distribution in the pore size seems to be more shifted to the right with pore size range of 120 and 190 nm and the frequency of the pores size at 130 nm is 33% [see Figure 6]. By using 4 wt.% PS in blend mixture, the distribution of the pore size is turned out to be in the range of 100 and 280 nm with the same pore size frequency at each of 100, 110, and 120 nm. Additionally, the distribution of

the pore size is appeared in the wide range (110 and 400 nm) at PS content of 6 wt. % in blend mixture. Pores in the size of about 130 nm have a frequency of 33%, the indication from these results can be confirmed that the distribution of the pore size of both surfaces are in the narrow range of all contents of PS in blend mixture. The truth of this phenomenon is due to the perfect physical mixing for DMAC solvent with the two polymers, owing to the character of non-polar PS and PVC as it has already been mentioned in the preceding sections.
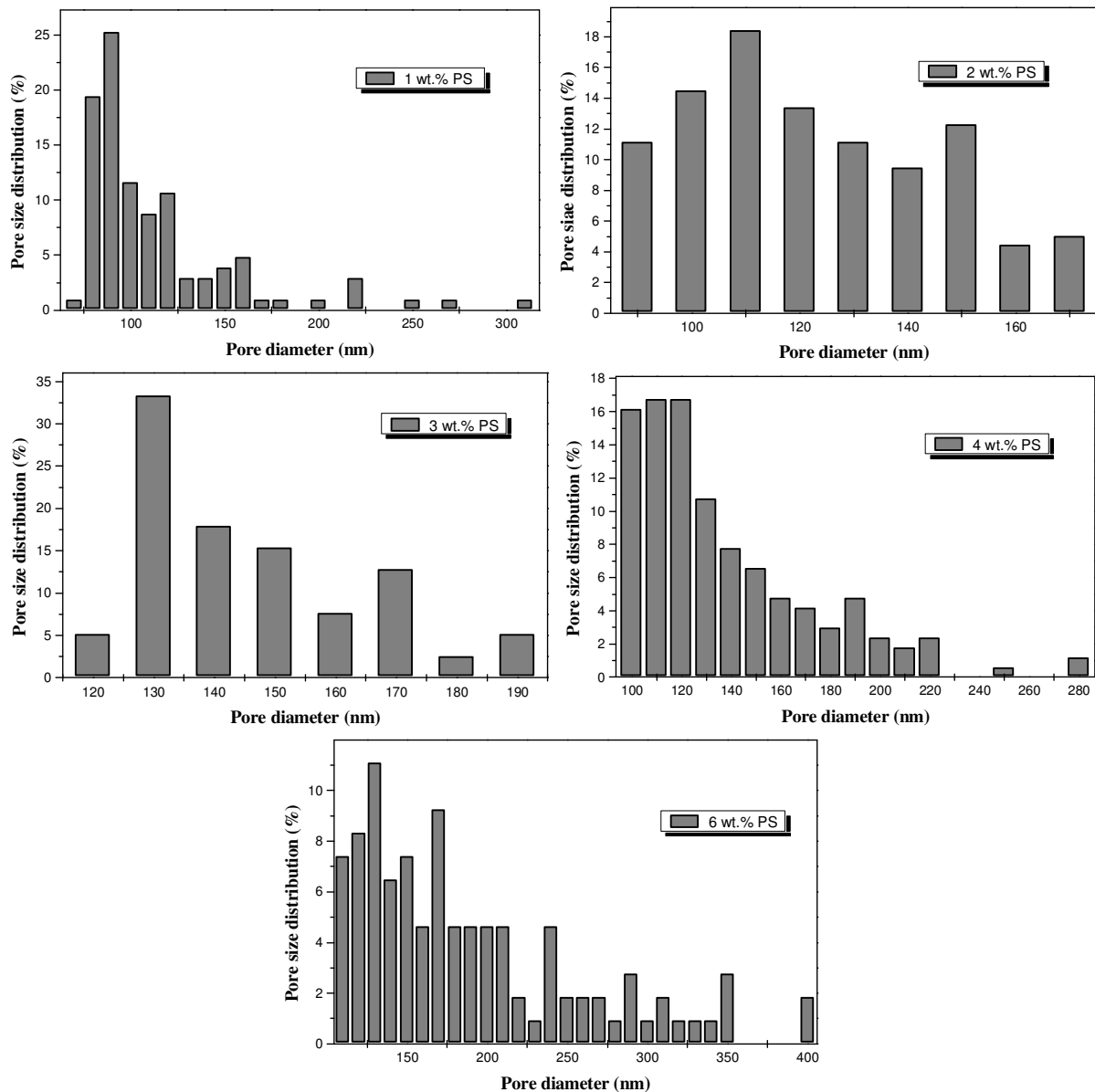
Fig. 6. Pore size distributions of the outer surface of the hollow fiber blend membranes.

Likewise, the cumulative distributions of pore sizes for both surfaces of the blend fibers are shown in Figure 7 and Figure 8. It is significant here to observe that the pore sizes cumulative distributions of outer and inner surfaces are moved toward the right side along with the increasing of PS contents in blend mixture. Here it should pay particular attention to the strong impact of the PS content on the dispersion of the pore size over the fibers surface. The observed phenomenon perhaps impute to the alteration in the rate of diffusion between the non-solvent in the internal and external coagulation baths and the solvent in the blend mixture. Table 1 and Table 2 summarized the mean roughness of the blend fibers in terms of R_m, R_{max} and R_a, for both surfaces of the blend fibers as a function of PS content in blend mixture. It can be

noticed that the results extracted from Tables show that an increase in the PS content inside the blend mixture leads to a decrease in the mean roughness of the blend surface. Knurl size of PS formed at both surfaces as a consequence of PS agglomeration can be fixed as a main factor of the mean roughness reduction in the blend fibers.

A good agreement of this watching was found in the results presented by Al-Salhy and co-workers [26]. Besides, Sotto and co-workers [27] had reported that as the PES content in casting solution increases, the roughness is decreased. The authors were found that a very compact nodule was formed with smooth surface as a reason of increasing the PES content.
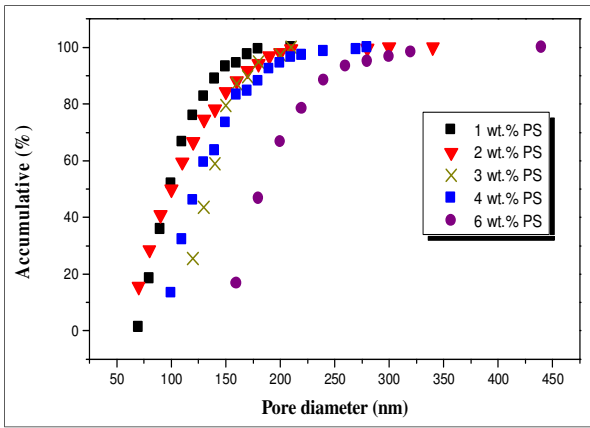
Fig. 7. Accumulative (%) of the pore diameter at the inner surface of the hollow fiber blend membranes.
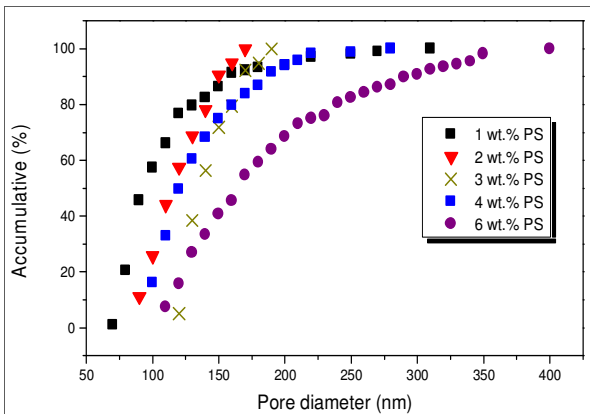

Fig. 8. Accumulative (%) of the pore diameter at the outer surface of the hollow fiber blend membranes.

3.3. Water Permeability

Finally, the influence of roughness of the outer surface of the blend fibers on the PWP is illustrates in Figure 9. From this Figure, it is perceived that as an increase the mean roughness of the outer surface, the PWP of blend fibers is increased. The behavior of this result is on account of the density expansion of the pores at the blend fiber surface as previously established in Figure 4. Accordingly, it is significant to deduce here the proportional relationship between the pore density and the mean roughness of the blend fibers that is sequentially influenced the blend fibers PWP. Chung et al. [17] discovered that the PWP of the PES fiber commensurate to the surface roughness.
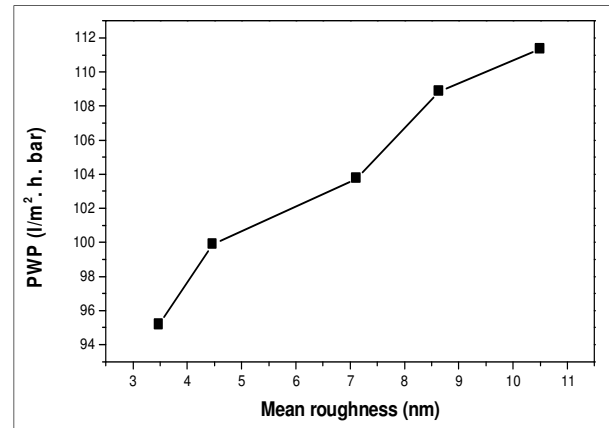

Fig. 9. Effect of mean roughness of the outer surface of hollow fiber membranes on the pure water permeability (PWP).

4. Conclusions

AFM-technique is used in this work for the purpose of analysis test the influence of PS concentration, as a second material, on the structure morphology and/or structure properties of the PVC fiber surfaces. The extracted conclusions can be summarized below:

- The polymer concentration in blend mixture has a major impact on the outer and inner surface morphology of PVC fibers.
- Noticeable a new nodules shape namely as "Crater nodules", is obtained at both outer and inner surfaces.
- Structure of the nodules is seen to be shifted from the nodules in the shape of Crater to stripe shape with increasing of the content of PS inside the blend mixture to about 6 wt.%. The behavior of this phenomenon is fundamentally because of the incorporation of the nodules of PS itself quicker than the nodules of PVC throughout the formation of blend fibers.
- Decreasing pore density and increasing mean size of the pores due to the increasing of the PS contents. This surveillance can be analyzed by means of the increase of the viscosity of the blend polymers mixture.
- From the extracted results it was detected that the size distribution of the pores of outer as well as inner surfaces seems to be narrow for all the used contents of PS owing to the perfect physical mixing of the DMAC with two polymers.
- Decrease of the mean roughness is due to the increase of PS content in blend mixture. This observation possibly because of the knurl of PS

formed on the surface as a result of the PS agglomeration.

• The PWP of the blend fibers is seen to be increased with increasing the outer surface roughness, which is caused by increment of blend fiber pore density.

Acknowledgements

5. References

[1] N. N. Li, A. G. Fane, W. S. Winston Ho, T. Matsuura, John Wiley & Sons, Inc., Hoboken, New Jersey, 2008.

[2] K.C. Khulbe, B. Kruczek, G. Chowdhury, S. Gagne, T. Matsuura, Surface morphology of homogeneous and asymmetric membranes made from poly (phenylene oxide) by tapping mode atomic force microscope, J. Appl. Polym. Sci. 59 (1996) 1151-1158.

[3] M. Hirose, H. Ito, Y. Kamiyama, Effect of skin layer surface structures on the flux behavior of RO membranes, J. Membr. Sci. 121 (1996) 209-215.

[4] J.Y. Kim, H.K. Lee, S.C. Kim, Surface structure and phase separation of polysulfone membrane by atomic force microscopy, J. Membr. Sci., 163 (1999) 159–166.

[5] M. Rafat, D. De, K.C. Khulbe, T. Nguyen and T. Matsuura, Surface characterization of hollow fiber membranes used in artificial kidney, J. Appl. Polym. Sci., 101 (2006) 4386–4400.

[6] J. Barzin, C. Feng, K.C. Khulbe, T. Matsuura, S.S. Madaeni, H. Mirzadeh, Characterization of polyethersulfone hemo-dialysis membrane by ultra-filtration and atomic force microscopy, Journal of Membrane Science 237 (2004) 77–85.

[7] N. Hilal, L. Al-Khatib, R. Al-Zoubi, R. Nigmatullin, Atomic force microscopy study of membranes modified by surface grafting of cationic polyelectrolyte, Desalination, 184 (2005) 45-55.

[8] K. Boussu, B. Van der Bruggen, A. Volodin, J. Snauwaert, C. Van Haesendonck, C. Van decasteele, Roughness and hydrophobicity studies of nano-filtration membranes using different modes of AFM, J. Colloid Interface Sci., 286 (2005) 632-638.

[9] J. A. Otero, O. Mazarrasa, J. Villasante, V. Silva, P. Pra´danos, J. I. Calvo, A. Herna´ndez, Three independent ways to obtain information on pore size distributions of nanofiltration membranes, J. Membr. Sci. 309 (2008) 17–27.

[10] S. A. Al-Malek, M.N. Abu Seman, D. Johnson, N. Hilal, Formation and characterization of polyethersulfone membranes using different concentrations of polyvinyl-pyrrolidone, Desalination 288 (2012) 31–39.

[11] K. Singh, P. G. Ingole, H. C. Bajaj, H. Gupta, Preparation, characterization and application of β-cyclodextrin-glutaraldehyde cross linked membrane for the enantiomeric separation of amino acids, Desalination, 298 (2012) 13–21.

[12] J. Stawikowska, A. G. Livingston, Assessment of atomic force microscopy for characterisation of nano-filtration membranes, Journal of Membrane Science, 425–426 (2013) 58–70.

[13] X.Y. Fu, T. Sotani, H. Matsuyama, Effect of membrane preparation method on the outer surface roughness of cellulose acetate butyrate hollow fiber membrane, Desalination 233 (2008) 10–18.

[14] A. M. El-Hadidy, S. Peldszus, M. I. Van Dyke Development of a pore construction data analysis technique for investigating pore size distribution of ultra-filtration membranes by atomic force microscopy, Journal of Membrane Science 429 (2013) 373–383.

[15] N. Faizah Razali, A. Mohammad, N. Hilal, C. Peng Leo, J. Alam, Optimization of polyethersulfone / polyaniline blended membranes using response surface methodology approach, Desalination 311 (2013) 182–191.

[16] M. A. Shirazi, D. Bastani, A. Kargari, M. Tabatabaei, Characterization of polymeric membranes for membrane distillation using atomic force microscopy, Desal. Water Treat., (2013) 1–6.

[17] T. Shung Chung, J. Jun Qin, A. Huan, K. Chua Toh, Visualization of the effect of die shear rate on the outer surface morphology of ultra-filtration membranes by AFM, Journal of Membrane Science 196 (2002) 251–266.

[18] Q. F. Alsalhy, Hollow fiber ultra-filtration membranes prepared from blends of poly (vinyl chloride) and polystyrene, Desalination 294 (2012) 44–52.

[19] S. Holger, V. G. Julius, Scanning Force Microscopy of Polymers, Springer Berlin Heidelberg, 2010.

[20] K. C. Khulbe, T. Matsuura, Characterization of synthetic membranes by Raman spectroscopy, electron spin resonance, and atomic force microscopy a review, Polymer, 41 (2000) 1917-1935.

[21] J. Brandrup, E. H. Immergut, Polymer Handbook [M], 3rd Edition Wiley, New York, 1989.

[22] J. Y. Lai, F. C. Lin, C. C. Wang, D. M. Wang, Effect of non-solvent additives on the porosity and morphology of asymmetric TPX membranes, J. Membr. Sci. 118 (1996) 49.

[23] R. E. Kesting, Synthetic Polymer Membranes, McGraw-Hill, New York, 1972.

[24] V. Thirtha, R. Lehman, T. Nosker, Morphological effects on glass transition behavior in selected immiscible blends of amorphous and semi-crystalline polymers, Polymer 47 (2006) 5392–5401.

[25] D. Wang, K. Li, W. K. Teo, Preparation and characterization of polyvinylidene fluoride (PVDF) hollow fiber membranes. J. Membr. Sci., 163(1999) 211-220.

[26] Q. F. Alsalhy, K. T. Rashid, S. S. Ibrahim, A. H. Ghanim, B. Van der Bruggen, P. Luis, M. Zablouk, Poly (vinylidene fluoride-co-hexafluoro propylene) (PVDF-co-HFP) Hollow Fiber Membranes Prepared from PVDF-co-HFP/PEG-600Mw/DMAC Solution for Membrane Distillation, J. Appl. Polym. Sci. (2013); published online DOI: 10.1002/app.39065.

[27] A. Sotto, A. Rashed, R. Xin Zhang, A. Martínez, L. Braken, P. Luis, B. Van der Bruggen, Improved membrane structures for seawater desalination by studying the influence of sub-layers, Desalination 287 (2012) 317–325.

أستقصاء مورفولوجيا السطوح المسامية بوساطة استخدام مجهر القوة الذري

بشير يوسف شرهان

قسم الهندسة الكيمياوية/ الجامعة التكنولوجية

البريد الالكتروني: bashiryoush1974123@yahoo.com

الخلاصة

يتعلق البحث بدراسة سطوح المواد المسامية وفحصها والتي تحتوي فتحات على سطحها تقود الى شبكة ذات ابعاد احادية او ثنائية او ثلاثية في داخل البناء الهيكلي لها وذلك باستخدام تقنية مجهر القوى الذري (AFM-technique). ان هذه التقنية تم استخدامها في البحث لدراسة تاثير محتوى البولي ستايرين على خواص السطوح الخارجية والداخلية لالياف البولى فنيل كلورايد المسامية عن طريق تغير مورفولوجيا السطح المسامي. وتم ملاحظة شكلاً لعقد مميز على السطوح الخارجية والداخلية عرفت علميا باسم: "Crater nodules".

حيث ان صور الالياف المستنبطة من خلا⬚ مجهر القوة الذري اوضحت ان تركيب العقد على السطوح الداخلية والخارجية كان منتظما عند استخدام محتوى قليل من البولي ستايرين. وعند تركيز 6% من مادة البولي ستايرين تم ملاحظة تغير الشكل الهيكلي للعقد من "Crater" الى "Stripe". ان زيادة محتوى البولى ستايرين ادى ايضا الى نقصان كثافة المسامات مع زيادة حجمهاعلى سطوح الالياف. الصور ثلاثية الابعاد لمجهر القوى الذري دلت كذلك على ان زيادة محتوى البولي ستايرين ادى الى نقصان خشونة السطوح الداخلية والخارجية لذلك فمعن⬚ نفاذية الماء عبر الالياف قل مع نقصان خشونة السطوح .